

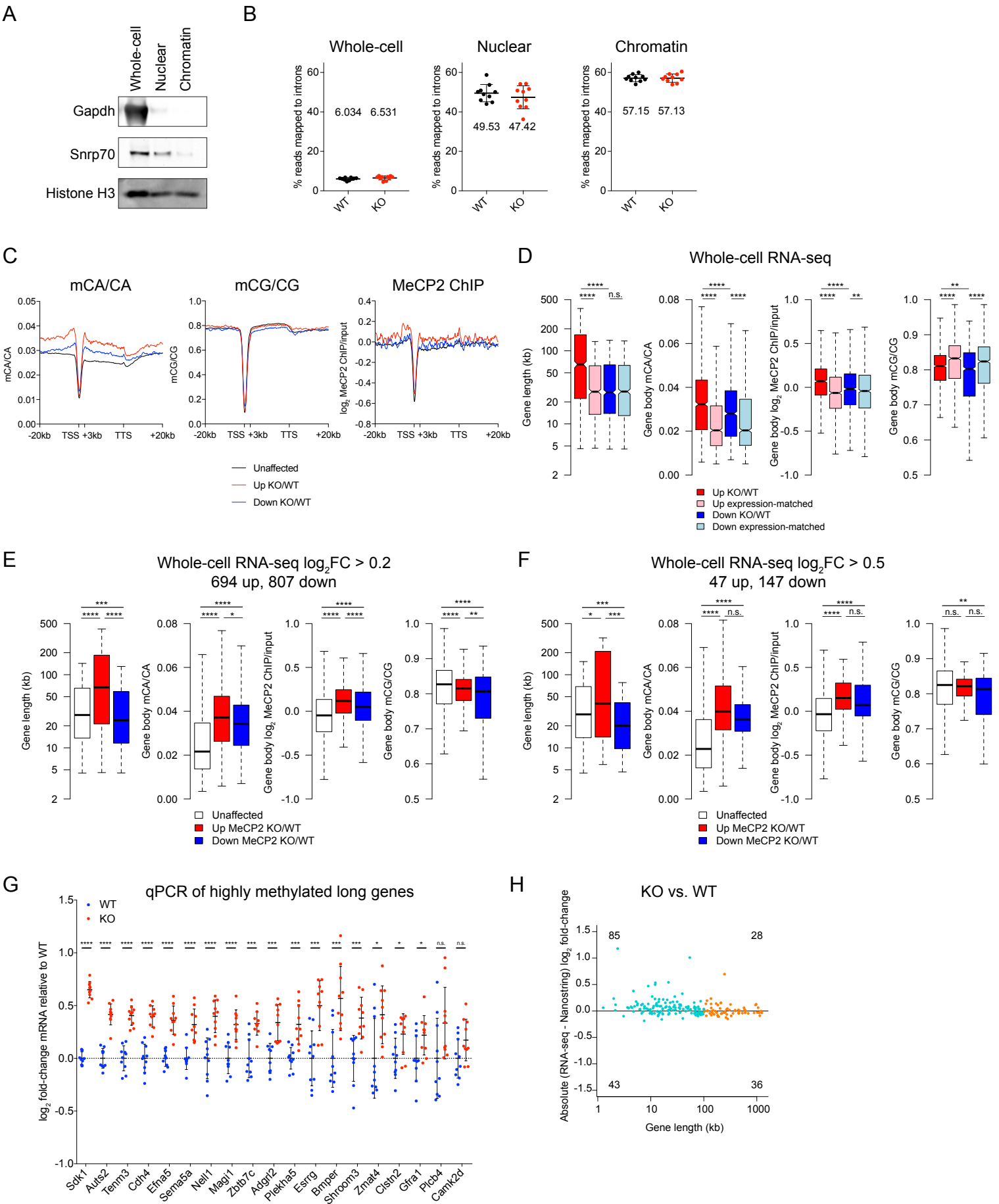
Molecular Cell, Volume 77

Supplemental Information

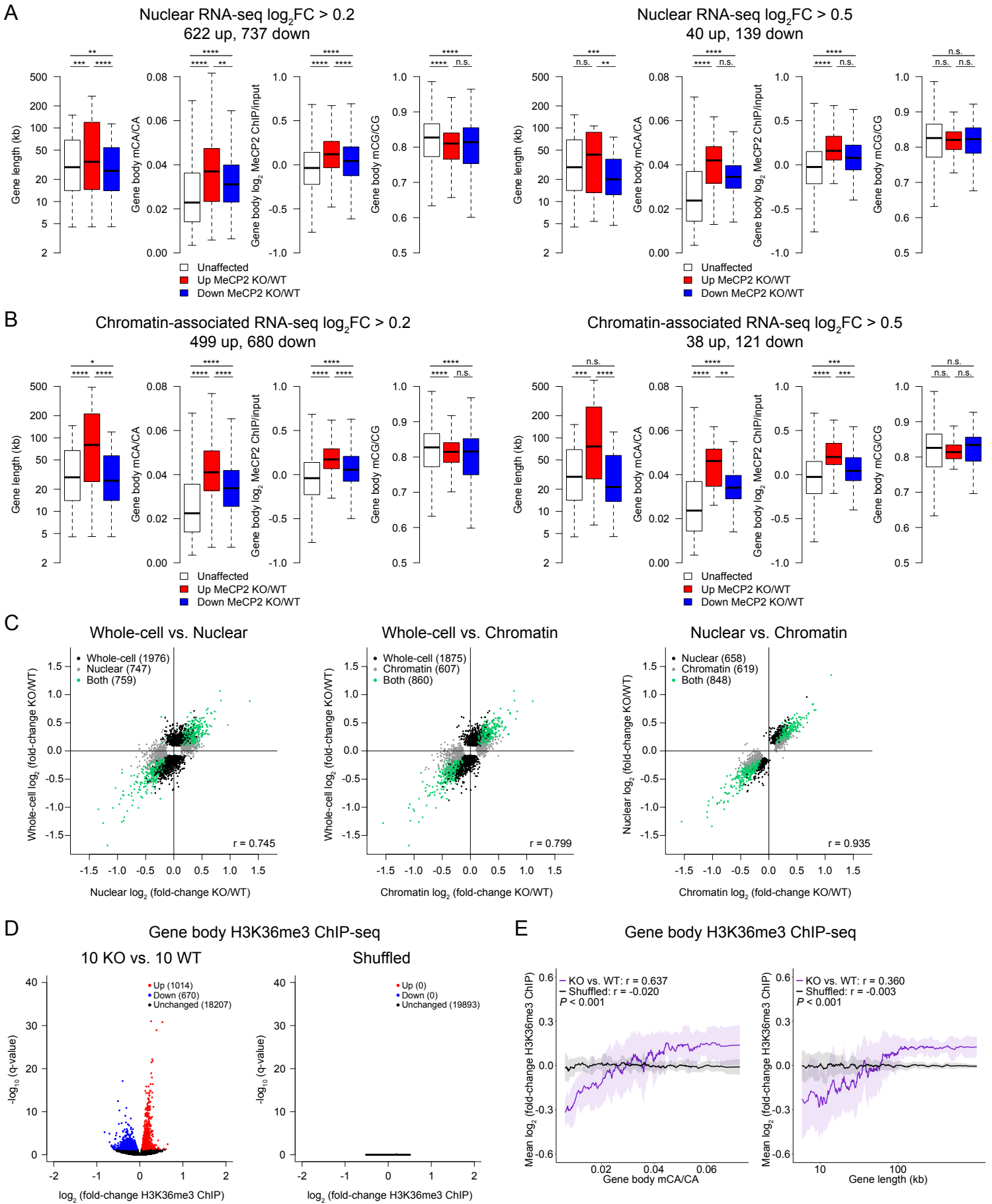
**MeCP2 Represses the Rate
of Transcriptional Initiation
of Highly Methylated Long Genes**

Lisa D. Boxer, William Renthall, Alexander W. Greben, Tess Whitwam, Andrew Silberfeld, Hume Stroud, Emmy Li, Marty G. Yang, Benyam Kinde, Eric C. Griffith, Boyan Bonev, and Michael E. Greenberg

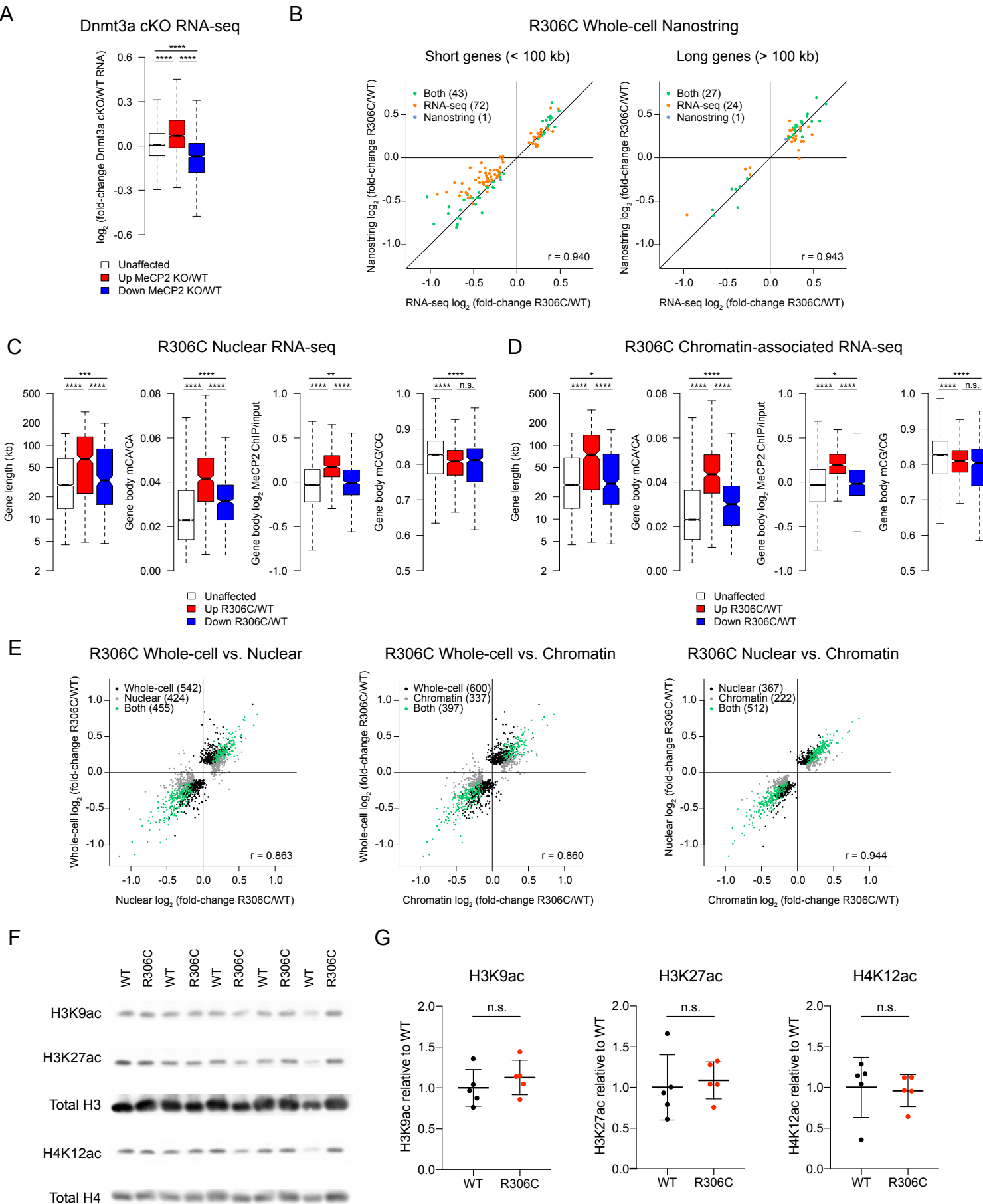
Supplemental Figure 1. Related to Figure 1.



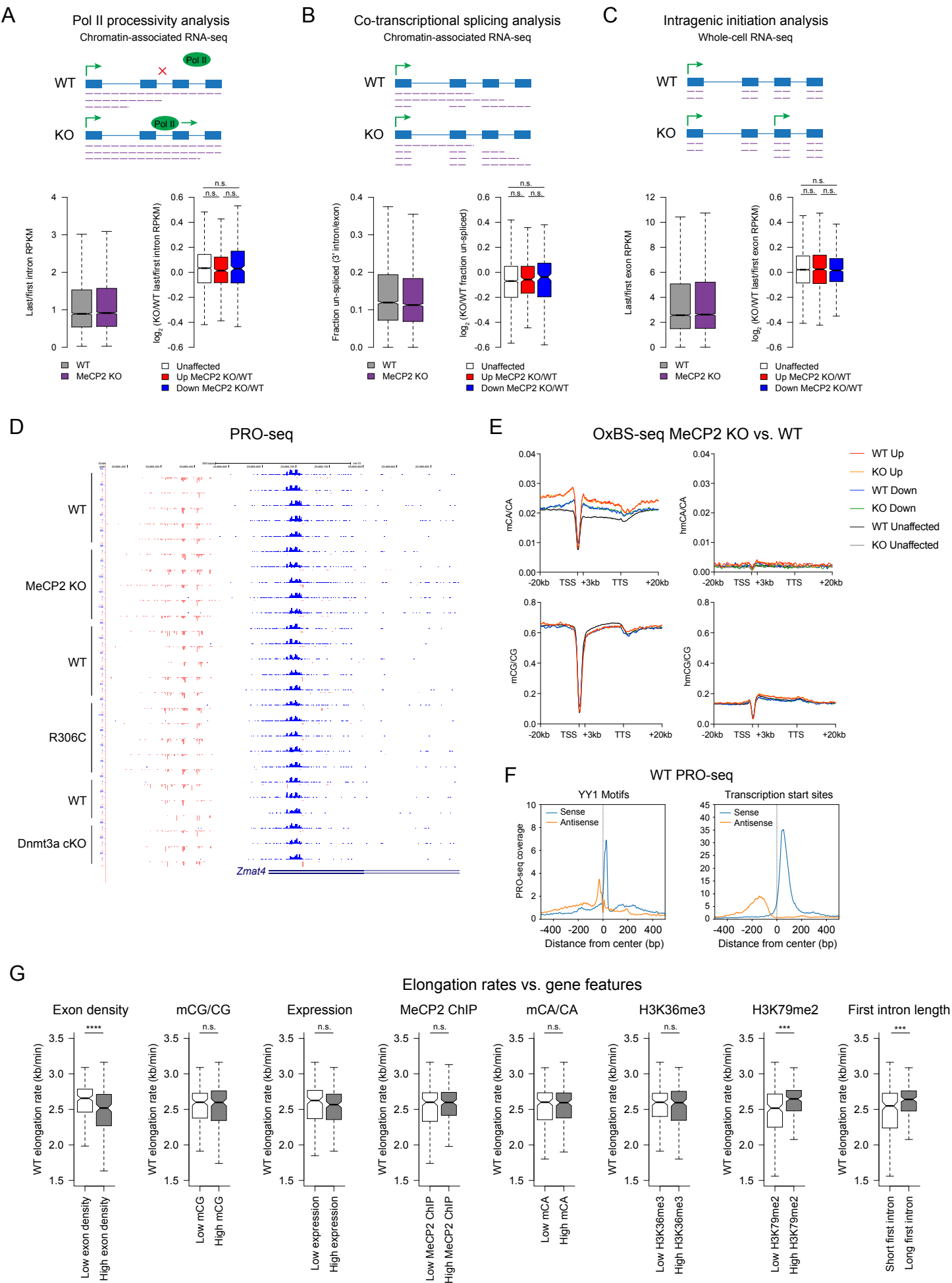
Supplemental Figure 2. Related to Figure 2.



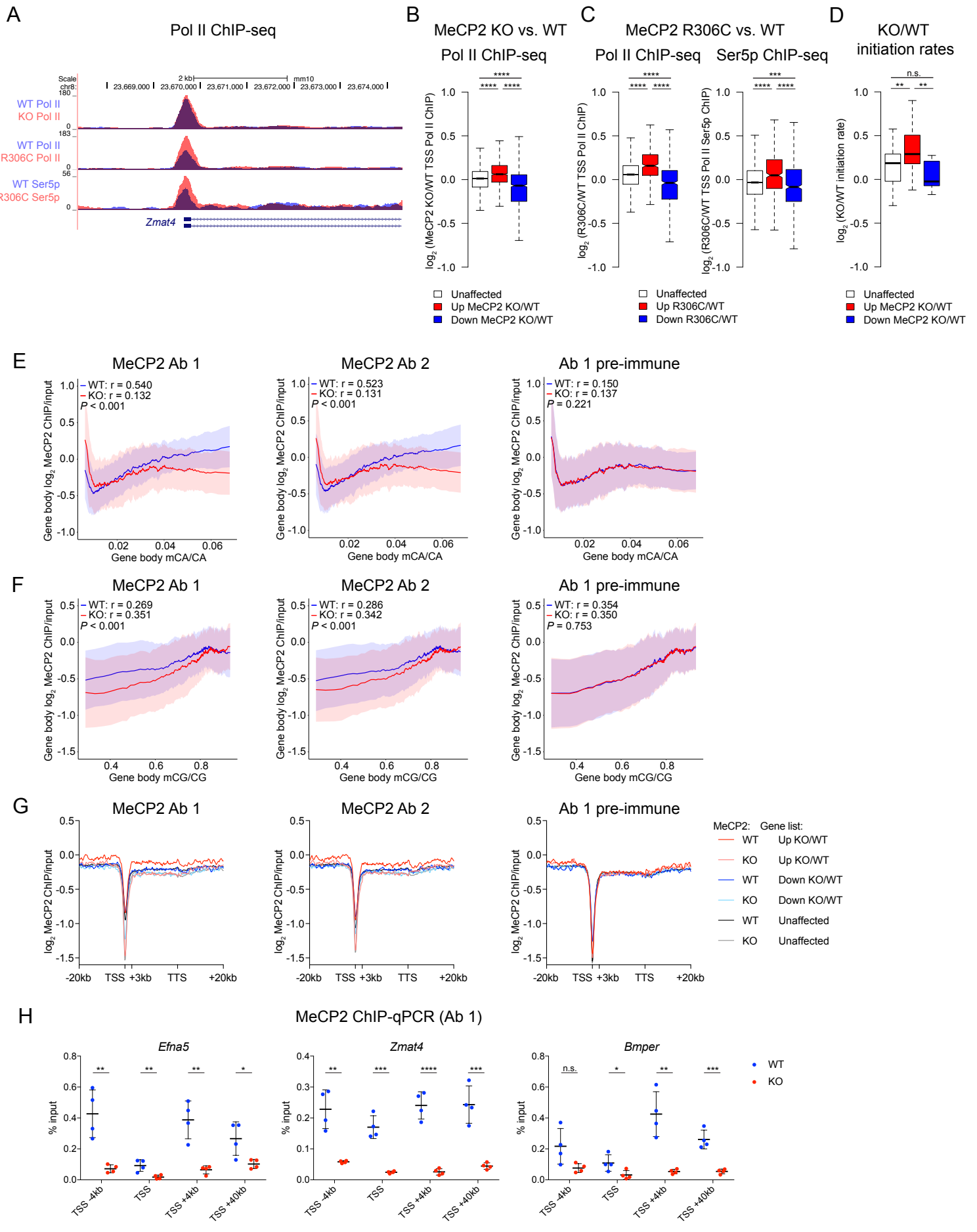
Supplemental Figure 3. Related to Figures 3 and 4.



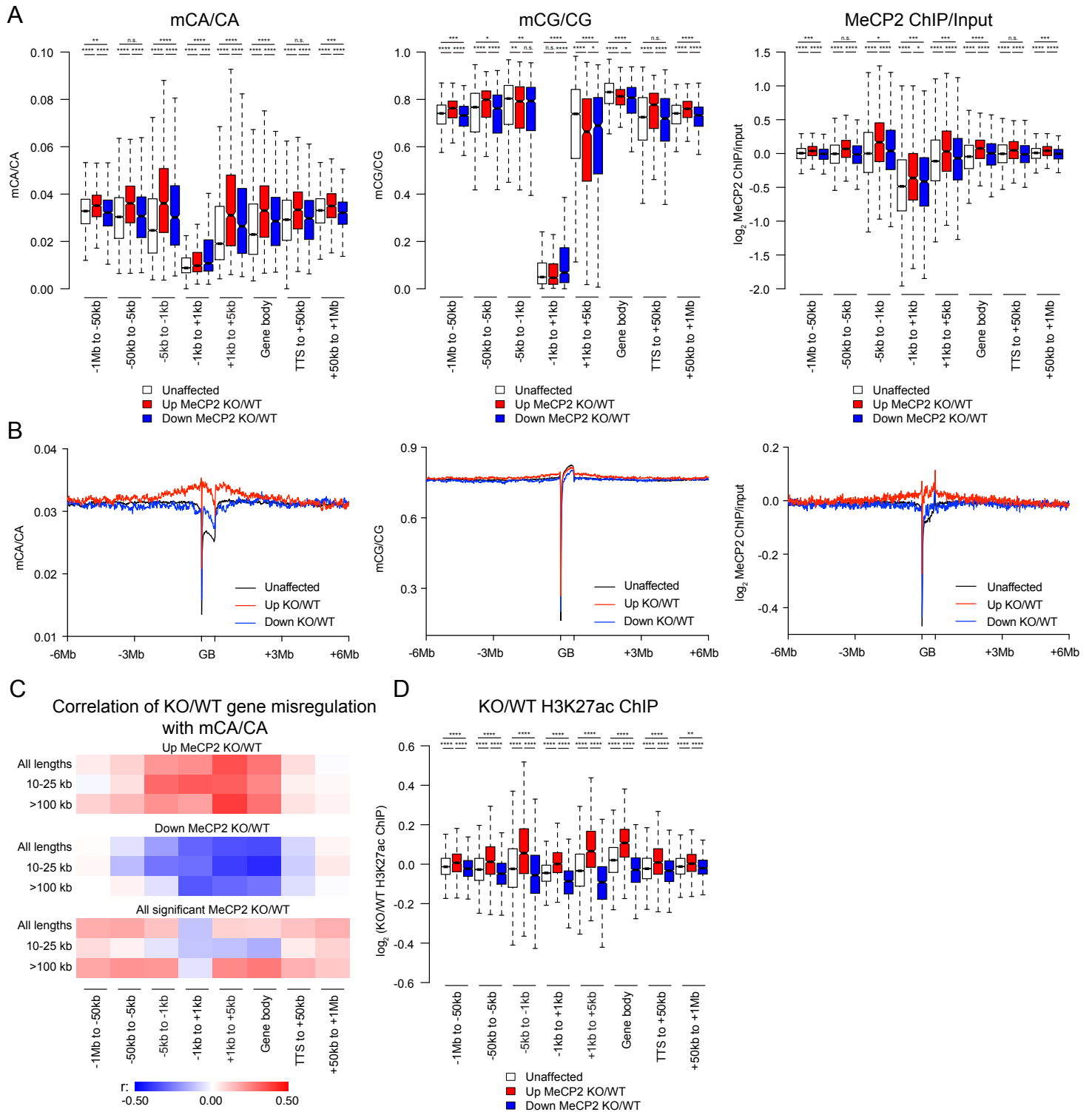
Supplemental Figure 4. Related to Figure 5.



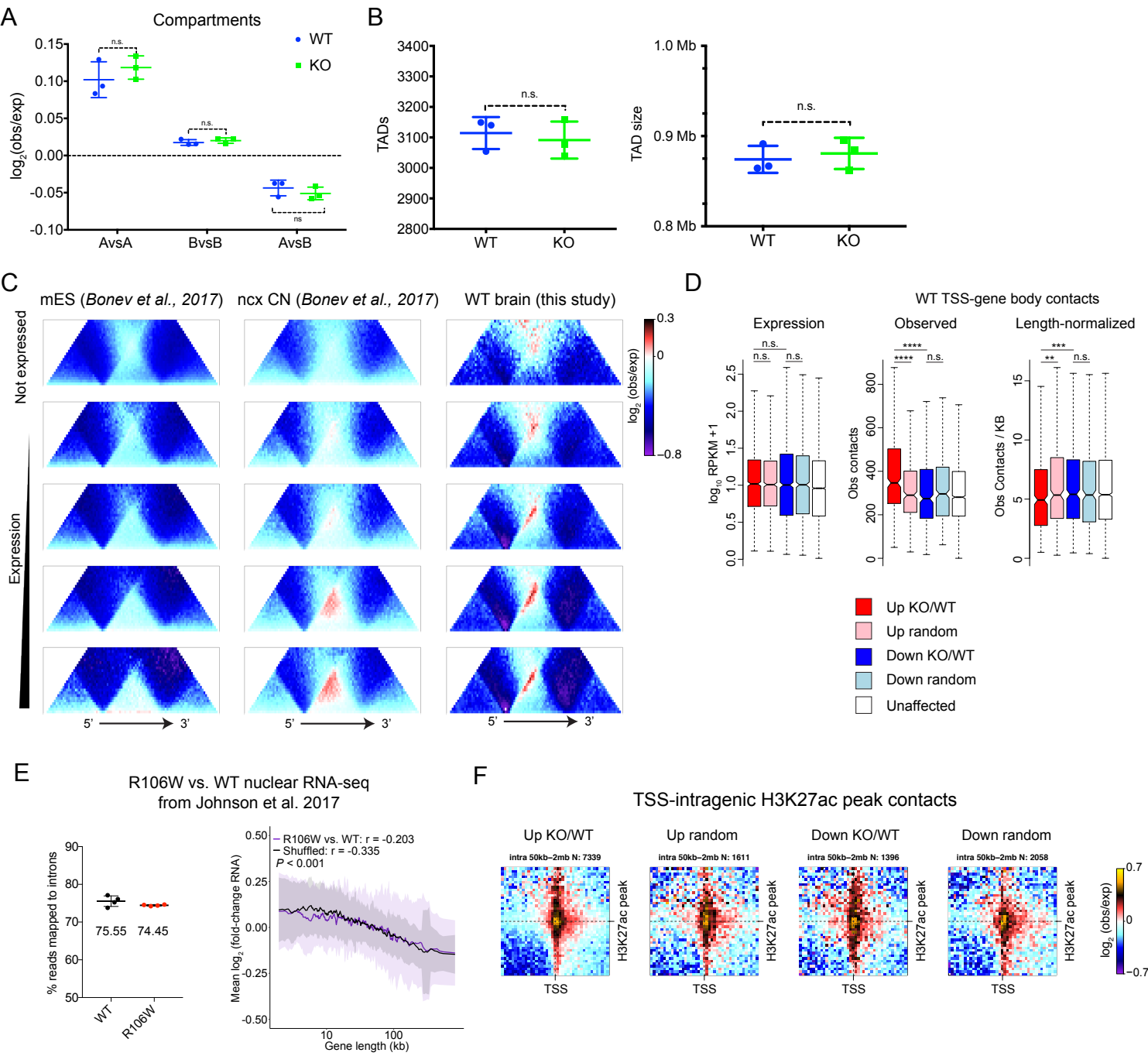
Supplemental Figure 5. Related to Figure 6.



Supplemental Figure 6. Related to Figure 6.



Supplemental Figure 7. Related to Figure 7.



SUPPLEMENTAL FIGURE LEGENDS

Supplemental Figure 1. Related to Figure 1.

A) Western blot of protein from whole-cell, nuclear, and chromatin-associated fractions with antibodies to the cytoplasmic protein Gapdh, soluble nuclear protein Snrp70, and chromatin-associated protein histone H3.

B) Percentage of RNA sequencing reads mapped to intronic regions in whole-cell (left), nuclear (middle), or chromatin-associated (right) RNA-seq from MeCP2 KO and WT.

C) Mean mCA/CA (left), mCG/CG (middle), and MeCP2 ChIP/input (right) across genes unaffected, up-regulated, or down-regulated in MeCP2 KO vs. WT whole-cell RNA-seq. Lines represent mean signal across genes in each list. The -20 kb to +3 kb and TTS to +20 kb regions are divided into 200 bp bins; TSS +3 kb to TTS is a metagene, with 100 equally sized bins per gene.

D) Boxplots of gene length, gene body mCA/CA, gene body MeCP2 ChIP/input, and gene body mCG/CG in genes up-regulated or down-regulated in MeCP2 KO vs. WT whole-cell RNA-seq compared to sets of expression-matched, unaffected genes. n.s. $P > 0.05$, ** $P < 0.01$, **** $P < 0.0001$. Kruskal-Wallis test with Dunn's post-hoc test.

E-F) Boxplots of gene length, gene body mCA/CA, gene body MeCP2 ChIP/input, and gene body mCG/CG in genes up-regulated, down-regulated, or unaffected in MeCP2 KO vs. WT whole-cell RNA-seq with a \log_2 fold-change (\log_2FC) > 0.2 (E) or $\log_2FC > 0.5$ (F). n.s. $P > 0.05$, * $P < 0.05$, ** $P < 0.01$, *** $P < 0.001$, **** $P < 0.0001$. Kruskal-Wallis test with Dunn's post-hoc test.

G) Quantitative PCR (qPCR) validation of 19 highly methylated long genes in 10 MeCP2 KO compared to 10 WT whole-cell RNA. n.s. $P > 0.05$, * $P < 0.05$, *** $P < 0.001$, **** $P < 0.0001$. Two-tailed unpaired t-test.

H) Absolute \log_2 fold-change difference between RNA-seq and Nanostring plotted against gene length. Orange dots depict long genes (> 100 kb), blue dots indicate short genes (< 100 kb). The absolute \log_2 fold-change difference between RNA-seq and Nanostring is negatively correlated with gene length (Pearson's $r = -0.163$, permutation test, $P = 0.001$), suggesting that, if anything, the MeCP2-dependent fold-changes are slightly overestimated for short rather than long genes by RNA-seq compared to Nanostring.

Supplemental Figure 2. Related to Figure 2.

A) Boxplots of gene length, gene body mCA/CA, gene body MeCP2 ChIP/input, and gene body mCG/CG in genes up-regulated, down-regulated, or unaffected in MeCP2 KO vs. WT nuclear RNA-seq with a \log_2 fold-change (\log_2FC) > 0.2 (left) or $\log_2FC > 0.5$ (right). n.s. $P > 0.05$, ** $P < 0.01$, *** $P < 0.001$, **** $P < 0.0001$. Kruskal-Wallis test with Dunn's post-hoc test.

B) Boxplots of gene length, gene body mCA/CA, gene body MeCP2 ChIP/input, and gene body mCG/CG in genes up-regulated, down-regulated, or unaffected in MeCP2 KO vs. WT chromatin-associated RNA-seq with a \log_2 fold-change (\log_2FC) > 0.2 (left) or $\log_2FC > 0.5$ (right). n.s. $P > 0.05$, ** $P < 0.01$, *** $P < 0.001$, **** $P < 0.0001$. Kruskal-Wallis test with Dunn's post-hoc test.

C) Correlation of KO vs. WT fold-change in gene expression between whole-cell and nuclear (left, $r = 0.745$), whole-cell and chromatin-associated (middle, $r = 0.799$), and nuclear and chromatin-associated (right, $r = 0.935$) RNA-seq data. There is significant overlap between the misregulated genes in the whole-cell and nuclear (up-regulated: $P = 8.61 \times 10^{-231}$, down-regulated: $P = 1.12 \times 10^{-140}$), whole-cell and chromatin-associated (up-regulated: $P = 1.64 \times 10^{-301}$, down-regulated: $P = 1.23 \times 10^{-200}$), and nuclear and chromatin-associated (up-regulated: $P < 1 \times 10^{-322}$, down-regulated: $P < 1 \times 10^{-322}$) datasets. P values calculated with Fisher's exact test.

D) Differential ChIP-seq analysis of gene body H3K36me3 ChIP-seq (TSS to TTS) from 10 MeCP2 KO vs. 10 WT (left) or 5 randomly selected WT and 5 randomly selected KO vs. the

remaining 5 WT and 5 KO samples (Shuffled, right). Significantly misregulated genes (FDR < 0.05) are shown in red (up-regulated) or blue (down-regulated).

E) The mean fold-changes of the genes with significantly misregulated gene body H3K36me3 ChIP-seq signal in MeCP2 KO vs. WT are displayed as a function of gene body mCA/CA (left) or gene length (right). The correlation between gene misregulation and mCA/CA was significantly greater in KO vs. WT than Shuffled (KO vs. WT, $r = 0.637$, Shuffled, $r = -0.020$, permutation test, $P < 0.001$). The correlation between gene misregulation and gene length was significantly greater in KO vs. WT than Shuffled (KO vs. WT, $r = 0.360$, Shuffled, $r = -0.003$, permutation test, $P < 0.001$). Lines represent mean fold-change in expression for 40 gene bins with 4 gene steps; ribbon is S.D. of each bin.

Supplemental Figure 3. Related to Figures 3 and 4.

A) Boxplot of fold-change in expression in Dnmt3a cKO compared to WT RNA-seq of genes significantly up-regulated, down-regulated, or unaffected in MeCP2 KO compared to WT whole-cell RNA-seq. **** $P < 0.0001$. Kruskal-Wallis test with Dunn's post-hoc test.

B) Correlation of fold-change in expression in R306C vs. WT assayed by Nanostring nCounter with fold-change in expression in R306C vs. WT assayed by RNA-seq for short genes (<100 kb, left, $r = 0.940$) or long genes (>100 kb, right, $r = 0.943$). Genes significantly misregulated (FDR < 0.05) in both Nanostring and RNA-seq are shown in green, genes significantly misregulated only in RNA-seq are shown in orange, and genes significantly misregulated only in Nanostring are shown in blue.

C-D) Boxplots of gene length, gene body mCA/CA, gene body MeCP2 ChIP/input, and gene body mCG/CG in genes up-regulated, down-regulated, or unaffected in R306C vs. WT nuclear RNA-seq (C), and R306C vs. WT chromatin-associated RNA-seq (D). n.s. $P > 0.05$, * $P < 0.05$, ** $P < 0.01$, *** $P < 0.001$, **** $P < 0.0001$. Kruskal-Wallis test with Dunn's post-hoc test.

E) Correlation of R306C vs. WT fold-change in gene expression between whole-cell and nuclear (left, $r = 0.863$), whole-cell and chromatin-associated (middle, $r = 0.86$), and nuclear and chromatin-associated (right, $r = 0.944$) RNA-seq data. There is significant overlap between the misregulated genes in the whole-cell and nuclear (up-regulated: $P = 9.01 \times 10^{-181}$, down-regulated: $P = 3.13 \times 10^{-260}$), whole-cell and chromatin-associated (up-regulated: $P = 3.58 \times 10^{-159}$, down-regulated: $P = 1.08 \times 10^{-228}$), and nuclear and chromatin-associated (up-regulated: $P < 1 \times 10^{-322}$, down-regulated: $P < 1 \times 10^{-322}$) datasets. P values calculated with Fisher's exact test.

F) Western blots from the visual cortex of MeCP2 R306C and WT mice for H3K9ac and H3K27ac compared to a total histone H3 loading control, and for H4K12ac compared to a total histone H4 loading control.

G) Quantification of western blots in (F). Histone acetylation signal is normalized to total histone signal for each sample and displayed as fold-change relative to the average WT. Histone acetylation levels are not significantly different between MeCP2 R306C and WT. n.s. $P > 0.05$. Two-tailed unpaired t-test.

Supplemental Figure 4. Related to Figure 5.

A) Analysis of Pol II processivity from chromatin-associated RNA-seq. Top: Schematic of expected results if there is increased Pol II processivity (decreased premature termination) in the MeCP2 KO compared to WT—increase in last/first intron RPKM in the KO compared to WT. Bottom left: Boxplots of average WT and average KO last/first intron RPKM for all genes with RPKM of at least 1 and at least 4 introns. No significant differences between KO and WT were detected by t-test after correcting for multiple comparisons (Benjamini-Hochberg, $Q=5\%$). Bottom right: Boxplots of \log_2 fold-change of (average KO last/first intron RPKM) compared to (average WT last/first intron RPKM) in genes unaffected, up-regulated, or down-regulated in MeCP2 KO vs. WT whole-cell RNA-seq. P values calculated with Kruskal-Wallis test with Dunn's post-hoc test (n.s. $P > 0.05$).

B) Analysis of co-transcriptional splicing from chromatin-associated RNA-seq. Top: Schematic of expected results if there is increased co-transcriptional splicing in MeCP2 KO compared to WT – decrease in the fraction of un-spliced transcripts, as measured by the 3' splice site ratio (last 25 bp of intron/first 25 bp of exon 3' to that intron). Bottom left: Boxplots of average WT and average KO fraction un-spliced for all genes a minimum coverage of 200 in the 25 bp exon region. No significant differences between KO and WT were detected by t-test after correcting for multiple comparisons (Benjamini-Hochberg, $Q=5\%$). Bottom right: Boxplots of \log_2 fold-change of average KO fraction un-spliced compared to average WT fraction un-spliced for 3' splice sites in genes unaffected, up-regulated, or down-regulated in MeCP2 KO vs. WT whole-cell RNA-seq. P values calculated with Kruskal-Wallis test with Dunn's post-hoc test (n.s. $P > 0.05$).

C) Analysis of spurious intragenic initiation from whole-cell RNA-seq. Top: Schematic of expected results if there is increased intragenic initiation in MeCP2 KO—increase in last/first exon RPKM in the KO compared to WT. Bottom left: Boxplots of average WT and average KO last/first exon RPKM for all genes with RPKM of at least 1 and at least 5 exons. No significant differences between KO and WT were detected by t-test after correcting for multiple comparisons (Benjamini-Hochberg, $Q = 5\%$). Bottom right: Boxplots of \log_2 fold-change of (average KO last / first exon RPKM) compared to (average WT last / first exon RPKM) in genes unaffected, up-regulated, or down-regulated in MeCP2 KO vs. WT whole-cell RNA-seq. P values calculated with Kruskal-Wallis test with Dunn's post-hoc test (n.s. $P > 0.05$).

D) Genome browser tracks of Precision Run-On sequencing (PRO-seq) from forebrain of MeCP2 KO ($n=5$), MeCP2 R306C ($n=5$), and Dnmt3a cKO ($n=3$) mice and their respective WT littermate controls.

E) Methyl-C and hydroxymethyl-C levels from OxBS-seq in MeCP2 KO compared to WT mice. Plots show mean mCA/CA (top left), hmCA/CA (top right), mCG/CG (bottom left), and hmCG/CG (bottom right) in MeCP2 KO and WT across genes unaffected, up-regulated, or

down-regulated in MeCP2 KO vs. WT whole-cell RNA-seq. Lines represent mean signal of three biological replicates. The -20 kb to +3 kb and TTS to +20 kb regions are divided into 200 bp bins; TSS +3 kb to TTS is a metagene, with 100 equally sized bins per gene.

F) Analysis of Pol II pausing at YY1 motifs and transcription start sites. Left: aggregate plots of WT PRO-seq read coverage centered on YY1 motifs (sense, blue, antisense, orange). YY1 motifs were obtained from YY1 ChIP-seq peaks derived from cortical neurons. Right: aggregate plots of WT PRO-seq read coverage centered on transcription start sites (sense, blue, antisense, orange). Lines show mean signal with 10 bp windows.

G) Boxplots of WT elongation rates for bottom 50% (low) compared to top 50% (high) of genes ranked for different gene features. Exon density is number of exons per kb; expression is RPKM from whole-cell RNA-seq. mCG/CG, mCA/CA, and MeCP2 ChIP/input levels are calculated from TSS +3kb to TTS, whereas H3K36me3 and H3K79me2 ChIP comprise the TSS to TTS. n.s. $P > 0.05$, *** $P < 0.001$, **** $P < 0.0001$. P values calculated with Wilcoxon rank-sum test.

Supplemental Figure 5. Related to Figure 6.

A) Genome browser tracks of Pol II or initiated Pol II (Ser5p) ChIP-seq from MeCP2 KO or MeCP2 R306C compared to WT forebrain ($n = 2$) for an example gene up-regulated in MeCP2-mutant compared to WT RNA-seq. The reads from replicates are combined and displayed as overlay tracks.

B) Boxplots of MeCP2 KO vs. WT Pol II ChIP-seq signal from -1 to +1 kb of the TSS of genes that are unaffected, up-regulated, or down-regulated in MeCP2 KO compared to WT whole-cell RNA-seq. **** $P < 0.0001$. Kruskal-Wallis test with Dunn's post-hoc test.

C) Boxplots of R306C vs. WT Pol II (left) or Pol II Ser5p (right) ChIP-seq signal from -1 to +1 kb of the TSS of genes that are unaffected, up-regulated, or down-regulated in MeCP2 R306C compared to WT whole-cell RNA-seq. *** $P < 0.001$, **** $P < 0.0001$. Kruskal-Wallis test with Dunn's post-hoc test.

D) Box plot of \log_2 fold-change in MeCP2 KO compared to WT initiation rate for genes with both measured elongation rates and initiation rates for genes unaffected (53 genes), up-regulated (29 genes), or down-regulated (7 genes) in MeCP2 KO compared to WT whole-cell RNA-seq. P values calculated with Kruskal-Wallis test with Dunn's post-hoc test. ** $P < 0.001$, n.s. $P > 0.05$.

E) Mean gene body ChIP/input from 2 WT and 2 MeCP2 KO forebrains with two different MeCP2 antibodies (left and middle) and the pre-immune serum for antibody 1 (right) displayed as a function of gene body mCA/CA. The correlation of MeCP2 ChIP with mCA/CA is significantly higher in WT than MeCP2 KO (MeCP2 Ab1: WT, $r = 0.540$, KO, $r = 0.132$, permutation test, $P < 0.001$; MeCP2 Ab2: WT, $r = 0.523$, KO, $r = 0.131$, permutation test, $P < 0.001$), but the correlation of pre-immune serum ChIP with mCA/CA is not significantly different in WT than MeCP2 KO (Pre-immune: WT, $r = 0.150$, KO, $r = 0.137$, permutation test, $P = 0.221$).

F) Mean gene body ChIP/input from 2 WT and 2 MeCP2 KO forebrains with two different MeCP2 antibodies (left and middle) and the pre-immune serum for antibody 1 (right) displayed as a function of gene body mCG/CG. The correlation of MeCP2 ChIP with mCG/CG is significantly lower in WT than MeCP2 KO (MeCP2 Ab1: WT, $r = 0.269$, KO, $r = 0.351$, permutation test, $P < 0.001$; MeCP2 Ab2: WT, $r = 0.286$, KO, $r = 0.342$, permutation test, $P < 0.001$), but the correlation of pre-immune serum ChIP with mCG/CG is not significantly different in WT than MeCP2 KO (Pre-immune: WT, $r = 0.354$, KO, $r = 0.350$, permutation test, $P = 0.753$).

G) Mean MeCP2 ChIP/input in WT and MeCP2 KO with MeCP2 Ab 1 (left), MeCP2 Ab 2 (middle), and Ab 1 pre-immune serum (right) across genes unaffected, up-regulated, or down-regulated in MeCP2 KO vs. WT whole-cell RNA-seq. Lines represent mean signal across genes in each list for 2 replicates. The -20 kb to +3 kb and TTS to +20 kb regions are divided into 200 bp bins; TSS +3 kb to TTS is a metagene, with 100 equally sized bins per gene.

H) ChIP-qPCR with MeCP2 antibody 1 from 4 WT and 4 MeCP2 KO forebrains with primers 4 kb upstream of TSS, TSS, 4kb downstream of TSS, and 40kb downstream of TSS (gene body) for 3 genes up-regulated in MeCP2 KO compared to WT. n.s. $P > 0.05$, * $P < 0.05$, *** $P < 0.001$, **** $P < 0.0001$. Two-tailed unpaired t-test. It should be noted that it remains possible that the MeCP2 ChIP signal we observe at the TSS comes from cross-linking gene body MeCP2 to the TSS rather than direct TSS binding given that there is significantly less mCA in this region. If true, it would suggest that the repressive effect of MeCP2 on initiation comes primarily from distant contacts between the gene body and TSS.

Supplemental Figure 6. Related to Figure 6.

A) Boxplots of mCA/CA (left), mCG/CG (middle), and MeCP2 ChIP/input (right) in various regions up- and downstream of gene bodies of genes that are unaffected, up-regulated, or down-regulated in MeCP2 KO compared to WT RNA-seq. Up-regulated genes show increased mCA levels in both TSS-flanking regions (-5 kb to -1 kb and +1 kb to +5 kb) and in a broader domain around genes (-1 Mb to -50 kb and +50 kb to +1 Mb). To distinguish TSS-flanking and gene body regions, only genes greater than 10 kb are included in the analysis, and gene body is defined as TSS +5 kb to TTS. n.s. $P > 0.05$, * $P < 0.05$, ** $P < 0.01$, *** $P < 0.001$, **** $P < 0.0001$. Kruskal-Wallis test with Dunn's post-hoc test.

B) Mean mCA/CA (left), mCG/CG (middle), and MeCP2 ChIP/input (right) in broad domains around genes unaffected, up-regulated, or down-regulated in MeCP2 KO vs. WT whole-cell RNA-seq. Lines represent mean signal across genes in each list. The -6Mb to TSS and TTS to +6 Mb regions are divided into 10 kb bins; GB (gene body) is a metagene, with 60 equally sized bins per gene. Genes greater than 10 kb in length are shown in the plots.

C) Heatmap of Pearson correlations of the fold-change in expression of genes significantly up-regulated (top), genes significantly down-regulated (middle), or all significantly misregulated genes (bottom) in MeCP2 KO vs. WT whole-cell RNA-seq compared to mCA/CA levels in

various regions up- and downstream of gene bodies. It is important to note that we have separated the genes that are up-regulated and down-regulated in MeCP2 mutant mice for most of our analyses with regard to genomic features (e.g. gene length, mCA levels, MeCP2 binding, histone modifications). The genes up-regulated (top) or down-regulated (middle) in MeCP2 KO demonstrate that gene upregulation or downregulation best correlates with mCA near the TSS. However, if we combine both the up- and down-regulated genes together (bottom), we observe a complicated mixture of the MeCP2-dependent effects that dilutes or even reverses stronger correlations that are observed with the individual sets of genes. While most of our analyses do not mix up- and down-regulated genes, for historical reasons, our moving average plots do and therefore require careful interpretation. For example, because the genes up-regulated in MeCP2 KOs have significantly higher gene body mCA levels and are longer than the unaffected or down-regulated genes, moving average plots of MeCP2-dependent gene expression as a function of gene length or mCA are a mixture of up- and down-regulated genes until the longest or most highly-methylated bins, which are comprised primarily of up-regulated genes.

D) Boxplots of MeCP2 KO compared to WT H3K27ac ChIP-seq signal in various regions up- and downstream of gene bodies of genes that are up-regulated, down-regulated, or unaffected in MeCP2 KO compared to WT RNA-seq. In addition to the TSS and gene body, up-regulated genes show increased KO compared to WT H3K27ac levels in both TSS-flanking regions (-5 kb to -1 kb and +1 kb to +5 kb) and in a broader domain around genes (-1 Mb to -50 kb and +50 kb to +1 Mb). ** $P < 0.01$, **** $P < 0.0001$. Kruskal-Wallis test with Dunn's post-hoc test.

Supplemental Figure 7. Related to Figure 7.

A) Hi-C contact enrichment between domains of the same type (A versus A or B versus B) and different type (A versus B). Data are represented as a scatter dot plot showing the mean and standard deviation. Statistical significance is calculated using student's t-test. n.s. $P > 0.05$.

B) Number of TADs (left) and average TAD size (right) for MeCP2 WT and KO. Data are represented as a scatter dot plot showing the mean and standard deviation. Statistical significance is calculated using student's t-test. n.s. $P > 0.05$.

C) Aggregate Hi-C maps of observed/expected TSS-gene body contacts for genes between 50 kb and 2 Mb in length oriented 5' to 3' and divided into 100 bins in ES cells (left) and cortical neurons (middle) from (Bonev et al., 2017) compared to WT brain from this study (right) for genes not expressed (top row) or expressed genes ranked in four equal quantiles by expression (bottom 4 rows).

D) Box plots of expression (left), observed number of TSS-gene body contacts (middle), and length-normalized observed TSS-gene body contacts (right) for genes up-regulated or down-regulated in MeCP2 KO vs. WT whole-cell RNA-seq compared to sets of expression-matched, unaffected genes (Up random and Down random) and all unaffected genes. n.s. $P > 0.05$, ** $P < 0.01$, *** $P < 0.001$, **** $P < 0.0001$. Wilcoxon rank-sum test.

E) Re-analysis of Johnson et al. nuclear RNA-seq from MeCP2 R106W compared to WT excitatory neurons. Left: Percentage of RNA-seq reads mapped to intronic regions in WT and R106W. Right: Mean fold-change of all expressed genes displayed as a function of gene length for R106W compared to WT or Shuffled (2 WT and 2 R106W with lowest % introns compared to 2 WT and R106W with highest % introns). The correlation between gene misregulation and gene length was significantly more negative in the Shuffled than R106W vs. WT (Shuffled, $r = -0.333$, R106W vs. WT, $r = -0.207$, permutation test, $P < 0.001$). Lines represent mean fold-change in expression for 200 gene bins with 40 gene steps; ribbon is S.D. of each bin. We note that in the mouse model reported in Johnson et al. a C-terminal epitope tag was fused to the WT and mutant forms of MeCP2. The addition of the epitope tag to otherwise wild-type MeCP2 in these mice led to a ~40% decrease in MeCP2 protein expression when compared to untagged WT MeCP2. This could in principle have resulted in changes in gene expression in the control mice that might have complicated subsequent comparisons to neurons expressing

mutant forms of MeCP2. In addition, it can be seen in this figure that the MeCP2-mutant nuclear samples used in the Johnson et al. study have a reduced total number of intronic reads compared to the WT nuclear samples, an effect that may be strong enough to account for the observed decreased expression of long genes in MeCP2-mutant nuclei, given that the negative correlation with gene length is also observed when samples are grouped by % introns rather than genotype. This overall difference in intronic read number between WT and R106W mice seems unlikely to be due to a direct reproducible effect of MeCP2 loss on transcription, because in our study, while we do observe reduced intronic reads in MeCP2 KO compared to WT nuclear RNA-seq, we do not detect any differences in intron read number between MeCP2 KO and WT whole-cell or chromatin-associated RNA-seq samples (Figure S1B). We suspect that MeCP2-mutant nuclei may be more fragile than WT nuclei, and that the decrease in the number of intron reads in the MeCP2-mutant samples may be a consequence of enhanced leakage of nascent RNA transcripts from the MeCP2-mutant nuclei during their isolation.

F) Aggregate Hi-C maps between the TSS and intragenic H3K27ac peaks of genes up- or down-regulated in MeCP2 KO vs. WT whole-cell RNA-seq compared to sets of expression-matched, unaffected genes (Up random and Down random). Intragenic H3K27ac peaks between 50 kb and 2 Mb downstream of the TSS are included. Shown are 80x80 kb windows with a bin size of 2 kb. Note that while TSS-gene body contacts are most enriched in the center of H3K27ac peaks, contacts are enriched within the gene body outside of H3K27ac peaks as well.